

Phase transitions in frustrated XY model on a square lattice

M. H. Qin and X. Chen

Laboratory of Solid State Microstructures, Nanjing University, Nanjing 210093, China

J. M. Liu

Laboratory of Solid State Microstructures, Nanjing University, Nanjing 210093, China;

School of Physics, South China Normal University, Guangzhou 510006, China;

and International Center for Materials Physics, Chinese Academy of Science, Shenyang 110016, China

(Received 4 August 2009; revised manuscript received 1 October 2009; published 14 December 2009)

We study the phase diagram of a frustrated XY model with a nematic coupling (Δ) on the square lattice by means of Monte Carlo simulation. Besides the conventional magnetic-chiral phase, the phase diagram shows an obvious region in which the magnetism is algebraically ordered but the chirality remains disordered. In addition, in the large Δ region, a nematic-chiral phase without magnetic order is identified, which is similar to the phase found in the frustrated XY model on triangular lattice [J. H. Park, S. Onoda, N. Nagaosa, and J. H. Han, *Phys. Rev. Lett.* **101**, 167202 (2008)]

DOI: [10.1103/PhysRevB.80.224415](https://doi.org/10.1103/PhysRevB.80.224415)

PACS number(s): 61.30.Cz, 75.10.Hk, 05.10.Ln

I. INTRODUCTION

Symmetry breaking decides orders. The spontaneous breaking of continuous symmetry in magnetic systems leads to the magnetic order, such as ferromagnetic or antiferromagnetic order. However, this mechanism may not be always true and may fail in low-dimensional systems due to the thermal or quantum fluctuations.¹ For instance, the classical two-dimensional (2D) XY model cannot sustain long-range magnetic order even with trivial thermal fluctuations, and alternatively the so-called algebraic-magnetic (aM) order with Kosterlitz-Thouless (KT) transition may ensue.² On the contrary, the spontaneous breaking of discrete symmetry is still allowed.³ The spin liquids are typical states with no conventional magnetic order, and yet can show some nontrivial orders which break some hidden discrete symmetries due to the frustrated interactions, and thus can be scaled by the topological number. For instance, spin chirality is relevant with the spontaneous breaking of discrete Z_2 symmetry.⁴ The vector spin chirality (vSC) is defined as $\sim \langle \mathbf{S}_i \times \mathbf{S}_j \rangle$ with the spin \mathbf{S}_i at site i , which is odd under spatial inversion and is closely related to multiferroic behavior.⁵⁻⁸ Besides the vSC, there is another scalar spin chirality $\langle \mathbf{S}_i \times \mathbf{S}_j \times \mathbf{S}_k \rangle$, which breaks the time-reversal symmetry and parity, and is related to the noncoplanar spin order observed in nontrivial glass transitions.⁹⁻¹¹

A typical model which contains both continuous and discrete symmetries can give rise to fertile phase transitions. The 2D fully frustrated XY (FFXY) model is a typical representative with a continuous $U(1)$ symmetry associated with global spin rotations and a discrete Z_2 symmetry since the ground state is double degenerate.^{4,12} At low temperature (T), this model has both algebraic XY order and long-range vSC order. As T increases, a two-stage transition will occur in which the XY order and chiral order will be destroyed at T_{KT} and T_χ , respectively.¹³⁻¹⁶ In fact, the two transition temperatures are extremely close to each other, with T_χ slightly higher than T_{KT} , indicating that the chiral order is associated with the algebraic-magnetic order, although there does exist a narrow T range only with chiral order.

Based on these studies, Park *et al.* recently investigated the FFX model on a triangular lattice in which an antiferromagnetic coupling (Δ) is included. Their calculation showed that a phase with both aM order and chiral order (magnetic-chiral phase) can transform into a phase with algebraic-nematic (aN) order and chiral order (nematic-chiral phase) with increasing Δ at low T .¹⁷ In Fig. 1, a schematic illustration of the transition from magnetic-chiral phase to nematic-chiral phase is given. The spins within the same sublattice arrange along or against a certain direction as visually shown with red arrows (gray arrows) in Fig. 1(b), forms the nematic order. The chiral order in this novel nematic-chiral phase is induced by the broken Z_2 symmetry in the nematic phase. In fact, the transition from an algebraic-magnetic order to a nematic order in a regular XY model with the nematic coupling was discussed earlier in Ref. 18, where it was pointed out that the phase transition is associated with an Ising transition from an integer vortex pair excitation in the aM phase to an half-integer vortex pair excitation in the nematic phase.

One may notice that the frustration in the model studied in Ref. 17 is stemmed from the triangular lattice geometry, and may question that if there are some interesting phases in other frustrated magnetic systems in which the frustrations are induced by ingredients such as the exchange interaction other than the geometric frustration. However, as far as we know, few works on this subject have been reported. In order to make clear this question, we will study a FFX model with the nematic coupling on a square lattice. The phase

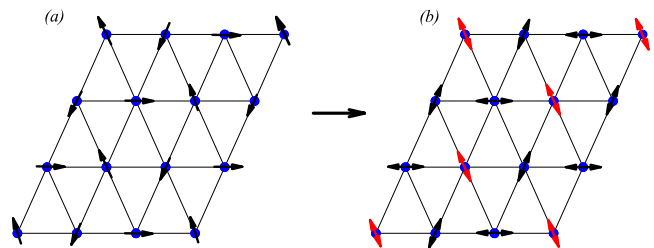


FIG. 1. (Color online) A schematic depiction of the transition from (a) magnetic-chiral phase to (b) nematic-chiral phase.

diagram obtained by means of Monte Carlo simulation shows a phase in which the magnetism is algebraically ordered but the chirality remains disordered over an extended T window. In addition, the nematic-chiral phase without magnetic order is also observed in the phase diagram, suggesting that our model as another classical spin model exhibits a vector chiral spin-liquid phase.

The remainder of this paper is organized as follows: In Sec. II the model and the simulation method will be described. Section III is attributed to the simulation results and discussion. At last, the conclusion is presented in Sec. IV.

II. MODEL AND METHOD OF SIMULATION

Here, we study a classical XY spin model on a square lattice. Different Hamiltonians for such a model were extensively investigated by rigorous and numerical approaches.^{18,19} We consider the following Hamiltonian which includes the frustration ingredient

$$H = -J_1 \sum_{[i,j]} \cos(\theta_i - \theta_j - A_{ij}) - J_2 \sum_{[i,j]} \cos(2\theta_i - 2\theta_j - A_{ij}), \quad (1)$$

where $0 \leq \theta_i < 2\pi$, indicates the spin orientation at site i , $[i,j]$ denotes the summation over all the nearest-neighbor spin pairs, $J_1 = 1 - \Delta$ the strength of the first coupling, $J_2 = \Delta$ the nematic coupling, the bond angle $A_{ij} = \pi$ or $-\pi$ for those bonds where both y_i and y_j , the y coordination of sites i and j , are odd, and $A_{ij} = 0$ elsewhere. For definition of the energy parameters J_1 and J_2 , the Boltzmann constant and also the lattice constant are set to unity. The $J_2 = 0$ limit was extensively studied due to its relevance with Josephson-junction arrays in a uniform transverse magnetic field, and it is believed to have the chirality transition at $T_\chi \approx 0.452$ and the KT transition at $T_{KT} \approx 0.446$.^{13-15,20-23}

Unlike the model studied in Ref. 19, which lacks the frustration ingredient, our model contains possible chiral orders induced by the frustration in the magnetic coupling. The ground state for our model is one in which the angular difference between the nearest neighbors is $\Phi_{ij} = \theta_i - \theta_j - A_{ij} = \pm \pi/4$ in the $J_2 = 0$ limit and $\Psi_{ij} = 2\theta_i - 2\theta_j - A_{ij} = \pm \pi/4$ in the $J_1 = 0$ limit. Therefore the two interactions are frustrated, and the ground state is decided by the competition between the two interactions, which is different from the model in Ref. 17 where no frustration exists between the J_1 and J_2 terms and the first term just lifts the degeneracy of the ground state of the second term.

Our simulation is performed on a 2D $L \times L$ ($L = 16, 24, 32, 40, 48, 64$) square lattice with period boundary conditions using the standard Metropolis algorithm and temperature exchange method.^{24,25} Here, the temperature exchange method is utilized in order to prevent the system from trapping in metastable free-energy minima caused by the frustration, if any. The initial spin configuration is totally disordered. Typically, the initial 1.5×10^5 Monte Carlo steps are discarded for equilibrium consideration and another 2×10^5 Monte Carlo steps are retained for statistic averaging of the simulation.

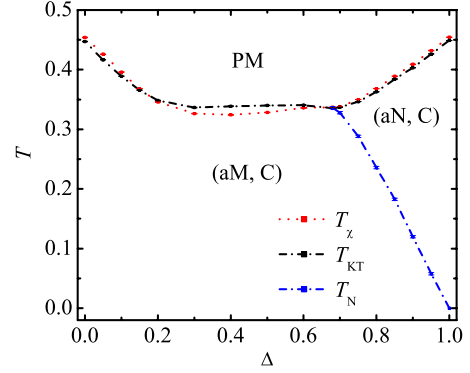


FIG. 2. (Color online) Calculated phase diagram for the model in Eq. (1). The high-temperature paramagnetic phase is denoted by PM, the phases with algebraic correlations in magnetic and nematic order by aM and aN, respectively, and the long-range correlations in the chirality order by C. The statistical errors of all the symbols are the same as their thickness in the T direction.

III. SIMULATION RESULTS AND DISCUSSION

A phase diagram in the Δ - T plane for the present model is constructed by the extensive simulation, and without any detailed analysis the simulated result is shown in Fig. 2. The three curves mark the boundaries between three different phases. The transition from the chiral (C) phase to the paramagnetic (PM) phase occurs at T_χ , and the transition from the algebraically correlated phase to the PM phase occurs at T_{KT} . As Δ increases, the transition from the aM order to the aN order occurs at T_N . In addition to the conventional magnetic-chiral order, our simulated result shows a obvious region in which the magnetism is algebraically ordered but the chirality remains disordered ($T_\chi < T_{KT}$). In the large Δ region, a nematic-chiral phase without magnetic order is observed, same as earlier report.¹⁷ In Sec. III A, we shall address separately these phase transitions in the phase diagram.

A. KT transition at T_{KT}

To determine T_{KT} , the point for the KT transition, we measure the helicity modulus, also called the spin-wave stiffness.^{4,26} For this case, the helicity modulus can be defined by

$$\begin{aligned} \Upsilon = & \frac{J_1}{L^2} \left\langle \sum_{[i,j]} x_{ij}^2 \cos(\theta_i - \theta_j - A_{ij}) \right\rangle \\ & + \frac{4J_2}{L^2} \left\langle \sum_{[i,j]} x_{ij}^2 \cos(2\theta_i - 2\theta_j - A_{ij}) \right\rangle \\ & - \frac{1}{TL^2} \left\langle \left[J_1 \sum_{[i,j]} x_{ij} \sin(\theta_i - \theta_j - A_{ij}) \right. \right. \\ & \left. \left. + 2J_2 \sum_{[i,j]} x_{ij} \sin(2\theta_i - 2\theta_j - A_{ij}) \right]^2 \right\rangle, \quad (2) \end{aligned}$$

where $x_{ij} = x_i - x_j$ is the separation of the x coordinates. For a given lattice size L , the KT transition point can be estimated by the crossing between the straight line $(2/\pi)(J_1 + 4J_2)T = (2/\pi)(1 + 3\Delta)T$ and the helicity modulus curve $\Upsilon(T)$. The

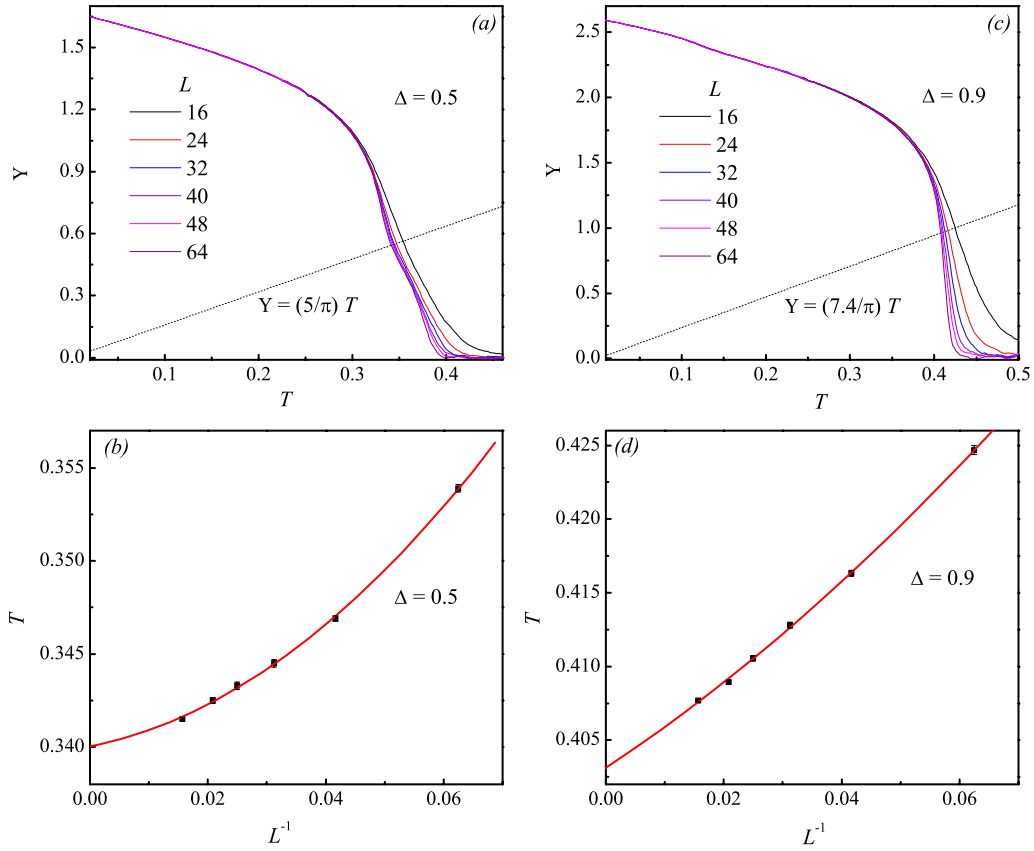


FIG. 3. (Color online) Helicity modulus Y as a function of T for various sizes L (a) at $\Delta=0.5$ and (c) $\Delta=0.9$. The straight line is $(2/\pi)(1+3\Delta)T$. The crossing temperatures of this line and Y for each L^{-1} are shown in (b) for $\Delta=0.5$ and (d) $\Delta=0.9$ with the extrapolation to $L^{-1}=0$.

helicity modulus for $L=16-64$ at $\Delta=0.5$ and 0.9 are plotted in Figs. 3(a) and 3(c), and the corresponding crossing points are shown in Figs. 3(b) and 3(d). In the bulk limit, the extrapolations using the polynomial fits give $T_{\text{KT}}=0.340(3)$ at $\Delta=0.5$ and $T_{\text{KT}}=0.403(1)$ at $\Delta=0.9$. This method has been approved to be effective in giving a good estimate of the KT transition temperature in some earlier works, and another method taking into account the logarithmic correction gives a similar result.^{17,23}

B. Chirality transition at T_χ

For the chirality transition, it is customary to study the staggered magnetization¹⁶

$$M = \frac{J_1}{L^2} \left| \sum_i (-1)^{x_i+y_i} m_{1i} \right| + \frac{2J_2}{L^2} \left| \sum_i (-1)^{x_i+y_i} m_{2i} \right|, \quad (3)$$

where the sum is over all the plaquettes of the system, $m_1 = \sin \Phi_{12} + \sin \Phi_{23} + \sin \Phi_{34} + \sin \Phi_{41}$ and $m_2 = \sin \Psi_{12} + \sin \Psi_{23} + \sin \Psi_{34} + \sin \Psi_{41}$ are the vorticities. For determining the phase-transition temperature, it is convenient to employ the Binder's fourth-order cumulant²⁷

$$U_L = 1 - \frac{\langle M^4 \rangle}{3\langle M^2 \rangle^2}, \quad (4)$$

where $\langle \dots \rangle$ is the ensemble average. For the usual cases where finite-size scaling applies, this quantity is size inde-

pendent at the critical point. So, the critical temperature T_χ can be obtained from the crossing of U_L for different L . As an example, the simulated U_L as a function of T at $\Delta=0.5$ and 0.9 for different lattice sizes are plotted in Fig. 4. From the well common defined crossing points shown in Figs. 4(a) and 4(b), we estimate $T_\chi=0.328(5)$ at $\Delta=0.5$ and $T_\chi=0.408(9)$ at $\Delta=0.9$.

As clearly shown in Fig. 2, T_χ stays slightly above T_{KT} in the small Δ range ($\Delta \leq 0.15$) and in the large Δ region ($\Delta \geq 0.7$), same as earlier report.¹⁷ In addition, the phase diagram contains two crossings of the KT transition and the chirality transition, as well as a certain Δ range in which T_{KT} stays well above T_χ . The identification of T_{KT} well above T_χ

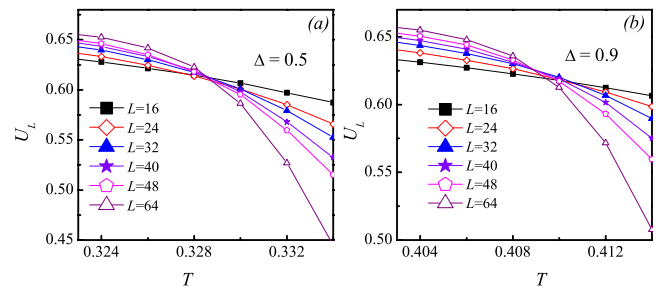


FIG. 4. (Color online) Binder's fourth-order cumulant U_L as a function of T for different lattice sizes at (a) $\Delta=0.5$ and (b) $\Delta=0.9$.

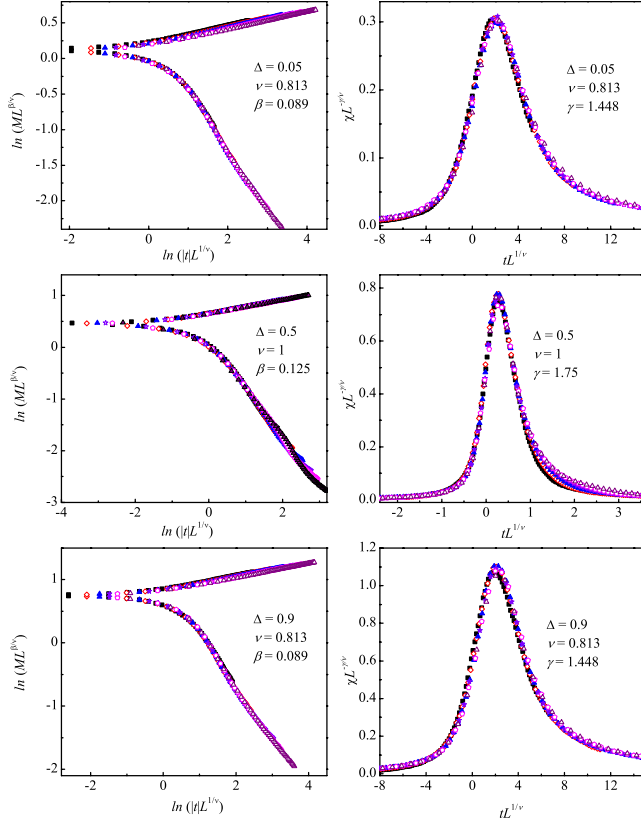


FIG. 5. (Color online) A scaling plot of M and its susceptibility χ for $\Delta=0.05$, $\Delta=0.5$, and $\Delta=0.9$.

proves the existence of the phase with only aM order in our model. In fact, the phase with only aM order has been observed in earlier work in which the phase diagram of the generalized FXY model on square lattice is studied in details.²³ It is identified that the chirality order disappears when p , the manipulated parameter of the interaction potential, becomes larger than its critical value p_c , due to the ground state in this region has no broken chirality symmetry. This result is different from our work where the chirality order exists in the whole Δ region. As analyzed earlier, the two terms (J_1 and J_2) of our model compete with each other for the formation of the chirality orders, while both of them contribute to the KT phase transition. Therefore in the middle Δ region, the chirality order can be significantly suppressed, leading to T_χ stays well below T_{KT} .

In Fig. 5, we plot the simulated M and its susceptibility, $\chi=(L^2/T)(\langle M^2 \rangle - \langle M \rangle^2)$, in the scaling form: $M=L^{-\beta/\nu}f(|t|L^{1/\nu})$, $\chi=L^{\gamma/\nu}g(tL^{1/\nu})$, with $t=(T-T_\chi)/T_\chi$, at $\Delta=0.05$, 0.5 , and 0.9 . It is observed that the chiral transition at these small sizes with the critical exponents $\nu=0.813(5)$, $\beta=0.089(8)$, and $\gamma=1.448(5)$ in the small Δ range ($\Delta \leq 0.15$) and in the large Δ region ($\Delta \geq 0.7$), consistent with earlier report at $\Delta=0$.¹⁴ However, recent research at large sizes [up to $L=O(10^3)$] at $\Delta=0$ has demonstrated that the chiral critical exponents are those of the 2D Ising model, i.e., $\nu=1$, $\beta=1/8$, and $\gamma=7/4$ which can be observed only after a pre-asymptotic regime.^{21,22} The non-Ising exponents obtained earlier have been thought of as an enhanced finite-size scaling effect at small sizes due to the screening length associated

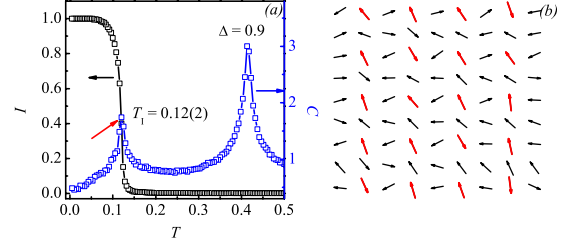


FIG. 6. (Color online) (a) Simulated curves of I and special heat C as a function of T at $\Delta=0.9$. (b) A snapshot of the nematic-chiral state at $T=0.2$ for $\Delta=0.9$. The spins in the same sublattice are shown with red arrows (gray arrows) for clarity.

with the nearby KT transition.¹⁵ On the other hand, in the middle Δ region ($0.2 < \Delta < 0.6$) where T_{KT} stays well away from T_χ , the finite-size scaling effect can be significantly weakened leading to the chirality transition with the exponents of 2D Ising model even at small sizes. So, it is likely that the non-Ising exponents obtained in this work are also effective ones and the true universality class of the chirality transition in the whole Δ region is that of 2D Ising transition.

C. Nematic transition at T_N

For $\Delta > 0.68$, a further transition from the aN phase to the aM one, which is associated with the transition from the integer vortex pair to the half-integer vortex pair, occurs at T_N . Following earlier work,¹⁷ the order parameter can be defined by

$$I = (4/L^2) \sum_{i \in B} \text{sgn}(\cos[\theta_i - \theta_{i_0}]), \quad (5)$$

where θ_{i_0} is the spin angle at some reference site i_0 of the sublattice B . Here, the site i in the sublattice B is selected with both odd x_i and y_i . In the nematic phase, θ_i and $\theta_i + \pi$ occur with equal probabilities, leading to a zero-order parameter I . In Fig. 6(a), parameter I and specific heat C as a function of T at $\Delta=0.9$ for $L=48$ are plotted. The sudden flop of I and the lower-temperature specific-heat peak at $T_N=0.12(2)$ clearly mark the nematic transition. However, the nematic transition cannot be scaled with the 2D Ising critical exponents, which may due to the frustrations in our system. As clearly shown in Fig. 2, this nematic transition occurs at a much lower temperature than either the chiral or the KT transition, leading to the existence of a nematic-chiral phase in which the chirality is ordered but the magnetism remains disordered. The chiral phase is induced by the breaking of Z_2 symmetry in the nematic transition as reported earlier. To some extent, our work proves that the same mechanism may hold true in some other similar frustrated systems. In Fig. 6(b), we show a snapshot of the nematic-chiral order at $T=0.2$ for $\Delta=0.9$. The spins within the same sublattice generally parallel or antiparallel with each other, as clearly shown with the red arrows. Therefore, apart from the FXY model on the triangular lattice, our model is another classical spin model which exhibits a vector chiral spin-liquid phase.

IV. CONCLUSION

In summary, we have studied the phase diagram of a frustrated XY model with a nematic coupling (Δ) on the square lattice using Monte Carlo simulation. The phase diagram for middle Δ exhibits a phase in which the magnetism is ordered but the chirality remains disordered, which is ascribed to the competition between the two couplings in the formation of the chirality order. For large Δ , the simulated result shows the existence of the nematic-chiral phase without any magnetic order, which qualifies our model as another classical

spin model that exhibits a vector chiral spin-liquid phase, in addition to the FFX Y model on the triangular lattice.

ACKNOWLEDGMENTS

This work was supported by the National Natural Science Foundation of China (Grants No. 50832002, No. 50601013, and No. 50528203) and the National Key Projects for Basic Researches of China (Grants No. 2009CB929501 and No. 2006CB921802).

-
- ¹N. D. Mermin and H. Wagner, Phys. Rev. Lett. **17**, 1133 (1966).
²J. M. Kosterlitz and D. J. Thouless, J. Phys. C **6**, 1181 (1973).
³R. B. Griffiths, Phys. Rev. **136**, A437 (1964).
⁴D. H. Lee, J. D. Joannopoulos, J. W. Negele, and D. P. Landau, Phys. Rev. B **33**, 450 (1986).
⁵K. F. Wang, J.-M. Liu, and Z. F. Ren, Adv. Phys. **58**, 321 (2009).
⁶H. Katsura, N. Nagaosa, and A. V. Balatsky, Phys. Rev. Lett. **95**, 057205 (2005).
⁷M. Mostovoy, Phys. Rev. Lett. **96**, 067601 (2006).
⁸D. Khomskii, Phys. **2**, 20 (2009).
⁹H. Kawamura and D. Imagawa, Phys. Rev. Lett. **87**, 207203 (2001).
¹⁰L. W. Lee and A. P. Young, Phys. Rev. Lett. **90**, 227203 (2003).
¹¹D. X. Viet and H. Kawamura, Phys. Rev. Lett. **102**, 027202 (2009).
¹²J. Villain, J. Phys. C **10**, 1717 (1977).
¹³S. Teitel and C. Jayaprakash, Phys. Rev. B **27**, 598 (1983).
¹⁴S. Lee and K. C. Lee, Phys. Rev. B **49**, 15184 (1994).
¹⁵P. Olsson, Phys. Rev. Lett. **75**, 2758 (1995).
¹⁶S. Lee and K. C. Lee, Phys. Rev. B **57**, 8472 (1998).
¹⁷J. H. Park, S. Onoda, N. Nagaosa, and J. H. Han, Phys. Rev. Lett. **101**, 167202 (2008).
¹⁸D. H. Lee and G. Grinstein, Phys. Rev. Lett. **55**, 541 (1985).
¹⁹D. B. Carpenter and J. T. Chalker, J. Phys.: Condens. Matter **1**, 4907 (1989).
²⁰S. E. Korshunov, Phys. Rev. Lett. **88**, 167007 (2002).
²¹M. Hasenbusch, A. Pelissetto, and E. Vicari, Phys. Rev. B **72**, 184502 (2005).
²²M. Hasenbusch, A. Pelissetto, and E. Vicari, J. Stat. Mech.: Theory Exp. (2005) P12002.
²³P. Minnhagen, B. J. Kim, S. Bernhardsson, and G. Cristofano, Phys. Rev. B **76**, 224403 (2007).
²⁴D. P. Landau and K. Binder, *A Guide to Monte Carlo Simulations in Statistical Physics* (Cambridge University Press, Cambridge, England, 2005).
²⁵K. Hukushima and K. Nemoto, J. Phys. Soc. Jpn. **65**, 1604 (1996).
²⁶M. E. Fisher, M. N. Barber, and D. Jasnow, Phys. Rev. A **8**, 1111 (1973).
²⁷K. Binder, Phys. Rev. Lett. **47**, 693 (1981).